ResearchGate

See discussions, stats, and author profiles for this publication at: https://www.researchgate.net/publication/6550447

Structural Flexibility of the Nucleosome Core Particle at Atomic Resolution Studied by Molecular Dynamics Simulation

ARTICLE *in* BIOPOLYMERS · APRIL 2007

Impact Factor: 2.39 · DOI: 10.1002/bip.20690 · Source: PubMed

CITATIONS
38

READS
55

3 AUTHORS, INCLUDING:

Danilo Roccatano
University of Lincoln
103 PUBLICATIONS **2,318** CITATIONS

SEE PROFILE

Available from: Danilo Roccatano
Retrieved on: 22 January 2016

Structural Flexibility of the Nucleosome Core Particle at Atomic Resolution Studied by Molecular Dynamics Simulation

Danilo Roccatano, Andre Barthel, Martin Zacharias
School of Engineering and Science, International University Bremen, Campus Ring 1, D-28759 Bremen, Germany

Received 8 November 2006; revised 15 January 2007; accepted 17 January 2007
Published online 24 January 2007 in Wiley InterScience (www.interscience.wiley.com). DOI 10.1002/bip.20690

ABSTRACT:

Comparative explicit solvent molecular dynamics (MD) simulations have been performed on a complete nucleosome core particle with and without N-terminal histone tails for more than 20 ns. Main purpose of the simulations was to study the dynamics of mobile elements such as histone N-terminal tails and how packing and DNA-bending influences the fine structure and dynamics of DNA. Except for the tails, histone and DNA molecules stayed on average close to the crystallographic start structure supporting the quality of the current force field approach. Despite the packing strain, no increase of transitions to noncanonical nucleic acid backbone conformations compared to regular B-DNA was observed. The pattern of kinks and bends along the DNA remained close to the experiment overall. In addition to the local dynamics, the simulations allowed the analysis of the superhelical mobility indicating a limited relative mobility of DNA segments separated by one superhelical turn (mean relative displacement of approximately ±0.2 nm, mainly along the superhelical axis). An even higher rigidity was found for relative motions (distance fluctuations) of segments separated by half a superhelical turn (approximately ±0.1 nm). The N-terminal tails underwent dramatic conformational rearrangements on the nanosecond time scale toward partially and transiently wrapped states around the DNA. Many of the histone tail changes corresponded to coupled association and folding events from fully solvent-exposed states toward complexes with the major and minor grooves of DNA. The simulations indicate that the rapid conformational changes of the tails can modulate the DNA accessibility within a few nanoseconds. © 2007 Wiley Periodicals, Inc. Biopolymers 85: 407–421, 2007.

Keywords: nucleic acid flexibility; nucleosome dynamics; DNA packing; DNA structure and dynamics; histone–DNA interaction; histone tail motion flexibility

This article was originally published online as an accepted preprint. The "Published Online" date corresponds to the preprint version. You can request a copy of the preprint by emailing the Biopolymers editorial office at biopolymers@wiley.com

Correspondence to: Martin Zacharias; e-mail: m.zacharias@iu-bremen.de
Contract grant sponsor: Pacific Northwest National Laboratories, USA
Contract grant number: gc9593
Contract grant sponsor: VolkswagenStiftung
Contract grant number: I/80485
This article contains supplementary material available via the Internet at http://www.interscience.wiley.com/jpages/0006-3525/suppmat

WILEY InterScience® DISCOVER SOMETHING GREAT

©2007 Wiley Periodicals, Inc.

INTRODUCTION

The nucleosome forms the basic structural unit of the eukaryotic chromatin. The nucleosome core particle consists of 147 base-pairs (bp) of DNA wrapped in a left-handed superhelix 1.65 times around a histone octamer. The octamer is formed by two copies of the histone proteins H2A, H2B, H3, and H4.[1–4] Each nucleosome is connected to it neighbors by a linker DNA (~10–80 bp). Nucleosomes can associate to form compact higher-order fiber structures (diameter of ~30 nm) that are essential for the compaction of eukaryotic DNA.[5–9] The nucleosome structure is not static but can change in particular upon

modification of histone proteins and of DNA.[9–15] Regulation of gene expression, replication, and DNA repair processes are tightly coupled to transient structural changes in the chromatin and nucleosomes structures.[10–15] Post-translational covalent modification includes acetylation and methylation of lysine residues and methylation of DNA. Recently, many new modifications in particular of histone tails have been discovered.[11,12,16–19] Modified histone tails can recruit gene regulatory proteins and other signal transduction proteins to nucleosomes to mediate chromatin remodeling. However, histone modification may also have a direct influence of the DNA-binding properties of the histone proteins.[20] The acetylation of lysine residues reduces the positive charge of histone proteins and may reduce the interaction with DNA. Access of buried regions in the nucleosome can be facilitated by recruitment of ATP-driven remodeling factors in response to a certain histone modification state.[5–9,21] However, spontaneous unwrapping is also possible to transiently increase the accessibility for proteins.[14,15] Fluorescence resonance energy transfer (FRET) measurements indicate that under physiological conditions, partial unwrapping of the DNA from the histone core can occur spontaneously starting from the ends of the wrapped DNA.[15]

Nucleosome core particle structures have recently been determined to high resolution,[1–4] allowing a detailed understanding of the DNA and histone structure in the nucleosome and the interactions that contribute to DNA–histone complex formation. The nucleosomal DNA differs from known free B-DNA oligonucleotide structures in that it adopts a curved structure with the inner site contacting the histone octamer at several sites and the other side exposed to solvent.[3] The nucleosome crystal structures also provided insight into the sequence dependence of the helical DNA structure and global deformability. Crystallographic B-factors indicate a modulation of DNA flexibility by the contacts to the histone octamer. Solvent-exposed parts of the DNA have larger B-factors than the inner side of the DNA in contact with the histone proteins.[4] However, crystallographic B-factors give only a qualitative picture on the local mobility of DNA and proteins in the nucleosome and also do not provide insights into the dynamics of highly mobile parts of the structure such as the histone tail regions. In addition, sequence-dependent differences in the mode of nucleosomal DNA-bending have been observed in the X-ray structure varying between a smooth bending and local kinking of the DNA.[3] The distribution of distinctive sequence motifs that facilitate sharp bending and kinking of DNA is of critical importance for nucleosome formation and positioning on chromosomal DNA.[22] Analysis of dinucleotide probability distributions in known nucleosome-binding sites has recently resulted in a genomic code for nucleosome positioning that can explain ~50% of in vivo-observed nucleosome positions.[23] Are these bending and kinking patterns observed in the nucleosome X-ray structure stable or do they rapidly exchange with alternative bending patterns? Recent experimental and computational studies on short DNA loops indicate that kinking can occur in DNA spontaneously and reversibly to allow for sharp DNA-bending.[24,25] It is also not clear whether the packing strain on DNA promotes dynamic transitions of the nucleic backbone toward more noncanonical states (e.g. coupled changes in the ε and ζ backbone torsion angles such as B_{II} states or coupled α–γ dihedral transitions) that change the recognition properties of the nucleosomal DNA.

In the present study, a MD simulation starting from a high-resolution structure of a nucleosome particle including explicit ions and water has been performed to characterize DNA and protein motions on the 20 ns range. In contrast to a previous shorter simulation starting from a lower resolution nucleosome structure,[26] the present study includes the motion of N-terminal histone tails and the results were compared to a simulation of a "tail-less" nucleosome (N-terminal tails removed from the start structure). Nucleosome dynamics has also been studied in a recent shorter MD simulation study that employed an implicit (generalized Born) solvation model.[27] However, use of an explicit solvent model might be more appropriate, since many histone–DNA contacts are mediated by water molecules[4] and the structure and dynamics may also depend significantly on the presence of explicit ions.[4,28]

Beside of simulation studies at atomic resolution, nucleosomes dynamics and nucleosome–nucleosome interactions have also been investigated using various coarse-grained models.[29–35] These simulation approaches employ reduced bead model representations of nucleosome particles and histone tails in combination with empirical interaction parameters to reproduce experimental data on the dynamics of nucleosomes and nucleosome oligomerization. Coarse-grained simulations aim at better understanding nucleosome oligomerization and chromatin formation and how it is influenced by the flexibility of single nucleosomes. The present simulation study focuses on single nucleosome dynamics at atomic resolution and how it influences the fine structure of DNA, the superhelical DNA motion, and the dynamics of histones and histone tails. During the present explicit solvent simulations, the structures stayed on average close to the experimental start structure with average helical and backbone parameters in good agreement with the experiment. The simulations allowed us to characterize fluctuations of helical motions along the DNA and to extract flexible global degrees

of freedom of the nucleosomal DNA and its superhelical mobility. These may give hints on possible directions of motion that result in large scale remodeling of the nucleosome. In addition, significant rearrangements of the histone tail structure from fully solvent-exposed states to transiently stable states that filled part of the minor and major grooves of the DNA were observed. The simulations indicate that the accessibility of DNA may change very rapidly within a few nanoseconds. The influence of the tails was further investigated by comparison to simulations on nucleosomes with truncated histone tails. Although increased mobility in particular of both termini of the wrapped DNA was observed, tail removal did not lead to a disruption of the DNA–histone contacts on the MD time scale. The current study is a first step toward characterizing the dynamics of eukaryotic DNA in its natural (packed) state in complex with histone proteins at atomic resolution. The study goes beyond previous simulation studies of nucleic acids that primarily focused on the dynamics of isolated oligonucleotides. It is not expected that on the 20-ns time scale any major conformational changes of the nucleosome such as unfolding, remodeling, etc. occur. However, the characterization of the magnitude of atomic fluctuations, helical fluctuations, backbone fluctuations, superhelical dynamics in this time regime is of major importance to estimate the influence of packing on DNA dynamics and its possible influence on recognition by other proteins. The MD simulation at atomic resolution may also complement and help to parameterize and refine previous modeling efforts on nucleosome fibers and chromatin that are based on Brownian dynamics simulations of coarse-grained models.[29–35]

MATERIALS AND METHODS

Molecular Dynamics Simulations

Molecular Dynamics (MD) simulations were started from a recent high-resolution crystal structure of the nucleosome[3] (pdb-entry: 1KX5; 0.19 nm resolution). The crystallographic water molecules and 14 Mg^{2+} ions were included in the simulations. The Mg^{2+} ions replace the Mn^{2+} ions in the crystal structure. As suggested in the X-ray analysis of the nucleosome structure, the low abundance of Mn^{2+} in vivo relative to Mg^{2+} implies that Mg^{2+} is likely being the preferred metal ion at these crystallographically defined ion-binding sites. Both metal ions favor an octahedral coordination geometry and the structural conservation for the interchange on Mn^{2+} and Mg^{2+} is well known and exemplified by RNA and DNA polymerase structures.[36,37] Initial positions of 270 K^+ counter and 154 Cl^- co-ions were placed using the xleap module of the Amber8 (Assisted Model Building with Energy Restraints) package.[38] Four crystallographically defined Cl^--binding sites were taken from the X-ray structure. Potassium counter ions were used (instead of sodium counter ions) because KCl has also been used in the buffer for the X-ray structure analysis and corresponds to the monovalent ion that has the highest concentration in the cell nucleus. Approximately 67,000 TIP3P water molecules[39] were added to fill a cubic box of $\sim 16.0 \times 16.0 \times 11.0$ nm^3 and leaving at least 1 nm between solute atoms and the borders of the box. During the simulations, transient ion association to small clusters of up to ~10 ion pairs was observed. This might be an artifact of the current force field. However, no irreversible ion crystal formation was observed during the current simulation time scale. In case of the simulations on the nucleosome structure with truncated histone tails, the N-terminal tail sequences of H2a, H2b, H3, and H4 up to residues 14, 30, 35, and 30, respectively, were removed from the X-ray coordinates. Simulations on this structure (tail-less simulations) were run at two ion concentrations. One corresponded approximately to the same conditions as used for the full nucleosome (~150 m*M*; 82 Cl^-, 14 Mg^{2+} and 270 K^+ ions, ~81,000 TIP3P water molecules). The second tail-less simulation system was run at a reduced ion concentration of ~100 m*M* (only the 4 Cl^- ions from the X-ray structure, 14 Mg^{2+} and 192 K^+ ions, ~73,000 TIP3P waters). Initial energy minimization (2500 steps) of the systems was performed with the *sander* module of the Amber8 package and using the parm99 force field.[40] Following minimization, the system was gradually heated from 50 to 300 K with positional restraints (force constant: 50 kcal mol^{-1} $Å^{-2}$) on DNA and protein atoms over a period of 0.5 ns allowing water molecules and ions to move freely. The *Rattle* algorithm[41] was used to constrain bond vibrations involving hydrogen atoms, which allows a time step of 2 fs. The *pmemd* module was used for all MD simulations. A 0.9 nm cutoff for the short-range nonbonded interactions was used in combination with the particle mesh Ewald option[42] using a grid spacing of ~0.09 nm to account for long-range electrostatic interactions. During additional 0.5 ns, the positional restraints were gradually reduced to allow finally unrestrained MD simulation of all atoms over a subsequent total simulation time of 21 ns for the full nucleosome and the tail-less nucleosome structure at reduced ion concentration (termed tail-less low salt simulation). The simulation time was 18 ns in case of the tail-less nucleosome at the same ion concentration as for the full nucleosome simulation (tail-less simulation). Only the last 15 ns simulation time (12 ns in case of tail-less simulation) were used for analysis (6 ns unrestrained equilibration time). Solute coordinates were stored every 0.25 ps simulation time. Principal component analysis (PCA) of the covariance of atomic fluctuations was performed using the Gromacs software package.[43] The VMD (Visual MD)[44] program was used for visualization of trajectories and preparation of figures.

Analysis of Helical and Superhelical Structure and Flexibility

The nucleic acid backbone structure and the helical parameters with respect to a helical DNA axis of the generated structures were analyzed using the program Curves5.1.[45] In addition, an analysis of the DNA superhelical structure was performed. The analysis of the superhelical structure of nucleosomal DNA is based on a superhelical axis, which has been defined as the normal vector to the mean plane of DNA with respect to the Cartesian coordinates of all C_1' atoms. The mean plane and the superhelical axis were determined by solving the eigenvalue problem $\mathbf{C}a = \lambda a$ ($\mathbf{C}$, covariance matrix of atomic coordinates) that is equivalent to a PCA. The eigenvector n corresponding to the vector with lowest eigenvalue and represents

in the current study the superhelical axis, whereas the remaining two eigenvectors are the axis that determine the mean plane. Note, that it is also possible to define a superhelical axis based on a vector orthogonal to the mean plane defined by the end points of the local helical axis vectors associated with each base pair.[46] This was also calculated and compared to the definition based on C_1' atom positions indicating an average directional difference of less than 0.5%. The orientation of the major groove at each base-pair was determined by taking the vector product $\vec{v}_{MG} = \vec{u} \times \vec{v}_{C_1'-C_1'}$ of the normal vector u and the C_1'–C_1' vector $v_{C_1'-C_1'}$ at each base-pair. The normalized projection P of this vector onto the vector r_{bp} from the base-pair center to the superhelical axis yields a scalar expression of the major groove orientation at each base-pair. The major groove at a base-pair points toward the superhelical axis with $P > 0$, i.e., the angle between v_{MG} and r_{bp} is less than 90°. If the major groove points outwards, then $P < 0$ and the angle is larger than 90°, respectively. Because of the right-handed nature of B-DNA, the major groove direction turns from pointing toward the superhelical axis to being parallel with the superhelical axis in 5′-3′ direction of DNA and to being antiparallel in 3′-5′ direction.

The superhelical pitch per base-pair step was determined by the projection of the vector v_{bs} joining the centers of two consecutive base-pairs onto the superhelical axis vector, i.e. $p = \vec{n} \bullet \vec{v}_{bs}$. The sum of superhelical pitch over base-pair steps gives an estimate of the total superhelical rise. As an extension, the superhelical rise of base-pairs being on top of each other was calculated by adding their distances from the nucleosomal mean plane, which gives an estimate of the total superhelical pitch as well.

The local bending of the DNA helical axis was determined as the angle θ between the normal vectors of adjacent base-pairs that is equivalent to the local bending resulting from the *roll* and *tilt* angle of base-pair steps ($\theta = \sqrt{\rho^2 + \tau^2}$).

RESULTS AND DISCUSSION

Stability of the Nucleosome Structure During the Simulations

The nucleosome simulations were started from the recently solved structure 1KX5.[3] This structure has been solved to high resolution (0.19 nm) and consists of the histone octamer and 147-bp DNA and includes histone tails that in part contact neighboring nucleosomes in the crystal. The nucleosomal DNA as well as the core part of the histone proteins (excluding histone tails, see Experimental Procedures) stayed close to the experimental structure during the entire simulation (Figures 1A and 1B). In case of the simulations starting from the same structure but missing the histone N-terminal tails and a reduced ion concentration (see Experimental Procedures), a slightly larger deviation of the DNA from the experimental structure was observed (Figure 1A). The histone core regions showed a stable root mean square deviation (RMSD) after the initial 5 ns equilibration time. Each of the two (symmetry-related) histone copies showed similar conformational drift over the simulation time (Figure 1B) and similar fluctuations along the sequence (not shown). Because of flexible C-terminal tail regions overall larger fluctuations and conformational drift were found for both copies of the histone protein H2A compared to the other histone proteins (Figure 1B). Compared to other histones in the octamer, the two H2A copies are localized at the two solvent exposed sides of the nucleosome. This greater exposure may also contribute to the overall larger mobility compared to other histone proteins. The overall drift of the DNA structure from experiment is in the order of ~0.25 nm and reached a stable plateau after about 3 ns simulation time. Overall, the positional fluctuations of the DNA are larger than the average protein atom

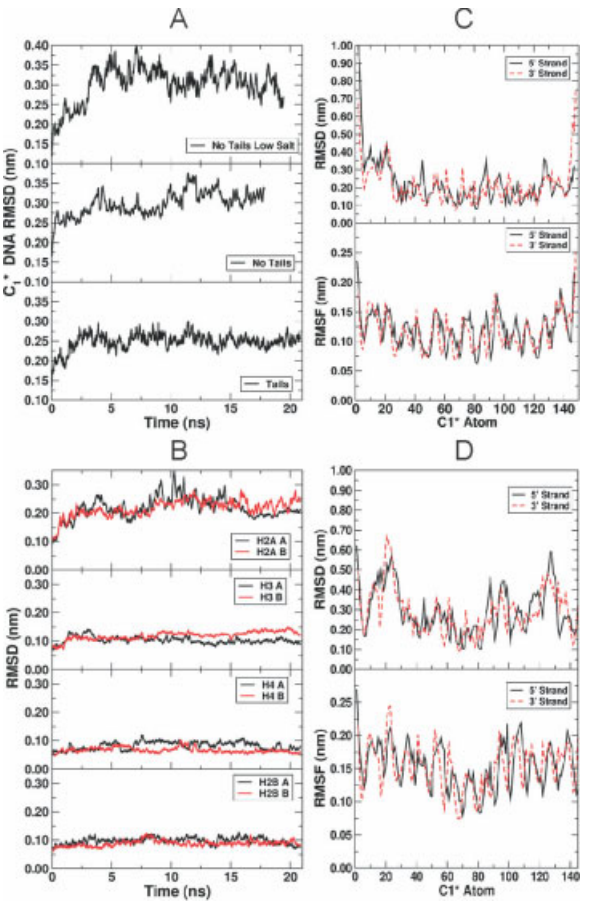

FIGURE 1 (A) RMSDs of the nucleosomal DNA versus simulation time. (B) Time courses of the histone protein backbone RMSD versus simulation time (showing only the heavy atom RMSD of the histone core residues excluding the N-terminal tail regions; see Materials and Methods). The RMSD of the individual histone chains are shown by different line types and colors as indicated in the insets of the plots. (C) Mean deviation from the X-ray structure (upper panel) and mean fluctuation of nucleotides during the data gathering period (5–21 ns) of the simulation including histone tails. (D) Same as in (C) but for the nucleosome simulation without tails at low salt.

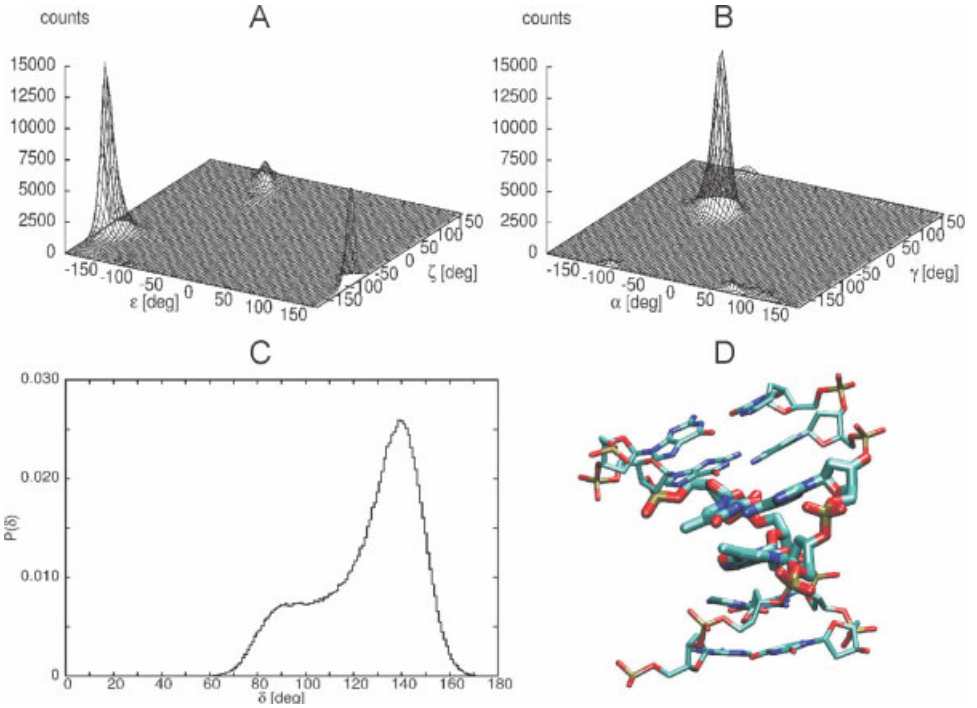

FIGURE 2 (A) Histogram for the observed distribution of backbone dihedral torsion angles ε/ζ (large/small peak indicates distribution of B_I/B_{II}-states) during the nucleosome MD simulation data gathering time. (B) Distribution of backbone dihedral torsion angles α and γ. (C) Distribution of dihedral torsion angles δ. (D) Example of a transiently observed DNA kinking at a pyrimidine/purine step (TA step at DNA position 50/51) and partial unstacking. The central TA step and two flanking base-pairs on both sides are shown.

fluctuations of the histone core (except for the histone tails discussed below) in agreement with the crystallographic B-factors.[4] The DNA side in contact with histone proteins in the nucleosome showed ~30–40% lower mobility than the solvent exposed parts of the DNA both for the simulations of the full nucleosome and without histone tails (Figures 1C and 1D). This leads to a characteristic periodic mobility pattern along the DNA sequence that qualitatively agrees with the B-factor pattern from the X-ray analysis (Figure 1 in the Supplementary Material).[4] Both strands of the DNA showed a very similar pattern of fluctuations indicating reasonable sampling of available conformational states around the X-ray structure on the nanosecond time scale. The increased RMSD shift and RMS fluctuations observed for the ends of the nucleosomal DNA (Figure 1C) indicates a tendency of the first and last 5 bp to transiently unwrap from the histone core. The DNA–histone interactions are dominated by electrostatic interactions between charged amino acid side chains and DNA phosphate groups and polar nucleobase groups at periodically spaced regions along the DNA.[3,4] These interactions remained stable during the current simulations of the complete nucleosome and also during the tail-less nucleosome simulations.

Nucleic Acid Backbone and Helical Fluctuations

The DNA backbone fine structure is mainly determined by the sugar pucker conformation as well as by the occurrence of coupled transitions of the α/γ (α/γ-flip) and ε/ζ (B_{II}-state) backbone dihedral angles, respectively (Figures 2A and 2B). In X-ray structures of B-DNA oligonucleotides, one typically finds ~7% A-form like sugar puckers (C_3'-endo instead of C_2'-endo) and a similar amount of B_{II} type ε/ζ dihedral states.[47] Recent systematic MD simulations (using also the Amber software) also indicate ~6% B_{II} type ε/ζ dihedral states for DNA oligonucleotides with many different sequences.[48] During the simulations, the great majority of nucleotides adopted standard B-type backbone conformations with few α/γ flips and B_{II} states (Figures 2A and 2B). It has been noted that α/γ flips can accumulate during very long MD-simulations on isolated DNA employing the Amber force field.[49] The nucleosome start structure contained already several nonstandard α/γ dihedral states (17: ~7%) with α in the +gauche or trans regime ($>30^\circ$) and γ near the trans regime ($> 120^\circ$ or $< -120^\circ$). Most of these α/γ flips persisted throughout the simulation with a small increase to 25 (~8.5%) toward the end of the simulation. It is likely that the packing constraints on the DNA in the nucleosome

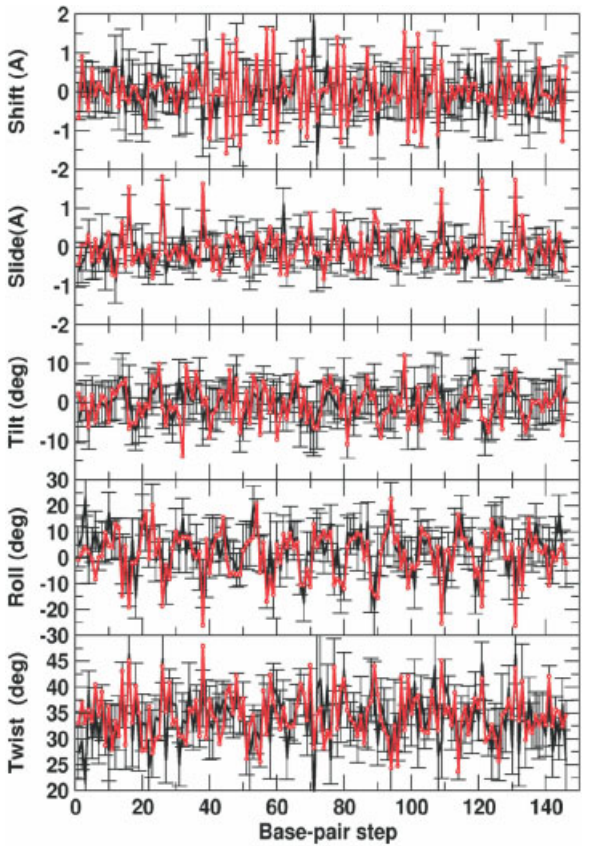

FIGURE 3 Helical parameter fluctuations during nucleosome simulation including histone tails. Average helical parameters observed during the data gathering period of the nucleosome simulation are indicated as black lines. The helical parameters extracted from the X-ray structure (pdb: 1kx5; Reference 3) are shown for comparison (red line). Observed helical parameter fluctuations (standard deviations) are indicated as error bars.

largely prevent transitions and a significant accumulation of α/γ flips that have been seen in simulations on isolated DNA oligonucleotides.[49] Approximately 5–10% of the nucleotides transiently adopt δ-dihedral angles around 85° more typical for A-form sugar conformations (Figure 2C). This is actually considerably smaller than what has been observed in systematic MD studies of isolated DNA oligonucleotides where more than 20% of the nucleotides adopted δ-dihedral angles smaller than 100°.[48] Overall, on the 20 ns time scale, the backbone dihedral structure of nucleosomal DNA is compatible with backbone dihedral distributions observed for experimental B-DNA type oligonucleotide structures. This supports the experimental result on the nucleosome core particle X-ray structure that the curved nucleosomal DNA structure is largely compatible with a standard B-DNA backbone structure.[3]

The average helical DNA parameters from the simulations are also in good agreement with data obtained from the X-ray analysis along the DNA (Figure 3). It is known that simulations of isolated DNA using the current Amber force field (parm99) result in a mean DNA twist of ~31–32°[48,49] that is smaller than the experimentally observed DNA twist of ~34.5° (in the nucleosome) or up to 36° in B-DNA crystal structures. During the nucleosome simulation, a slight reduction of the mean twist from 34.5° (start structure) down to 33.7° in the final structure of the simulation was observed. However, this is mainly due to DNA untwisting at the "free" (unpacked) ends of the nucleosomal DNA. The mean twist of the central DNA part (without the first and last 6 bp) was 34.4° in the start structure versus 34.2° in the final structure. It is likely that the packing of the DNA around the histone core prevents any further untwisting of the DNA, since it likely causes disruption of DNA–histone contacts.

The order of the helical parameter fluctuations follows qualitatively the order seen in MD simulations of isolated DNA[48] or distributions obtained from X-ray structures[47] (standard deviation of roll > twist > tilt; standard deviation of shift > slide > rise). However, the average fluctuation magnitude is ~20–30% larger than what has been reported for simulations on DNA oligonucleotides (e.g. average standard deviation of nucleosomal DNA twist: ~8° compared to ~6° for oligonucleotide simulations[48]). Very similar distributions of helical as well as backbone parameters have been observed for the simulations without histone tails (not shown). This agrees also with a previous shorter simulation on a nucleosome core particle based on an X-ray structure without complete histone tails that indicated a helical structure in agreement with experiment.[22] The X-ray analysis of the nucleosome structure showed that the DNA-bending is not uniformly distributed but different types of bends and kinks are formed along the nucleosomal DNA depending on the sequence.[3] Smooth bending toward the minor or major grooves characterized by a periodic and relatively smooth variation of roll and tilt is largely preserved during the simulations. In addition, kinked bending towards the major groove shows also up in the simulations that frequently involved partial unstacking and also an intrabase-pair distortion (e.g. a change in propeller twist as illustrated in Figure 2D). Most of the DNA-kinks observed during the simulations stayed close to the positions seen in the X-ray start structure with the exception of regions near the ends of the DNA with for example larger changes in the roll angle (Figure 3). A kinked minor groove motif already observed in the X-ray structure at several pyrimidine/purine (Py/Pu) dinucleotide steps[3] associated with a significant local positive change in the helical variable slide coupled to a large negative roll and decreased twist was also observed during the MD

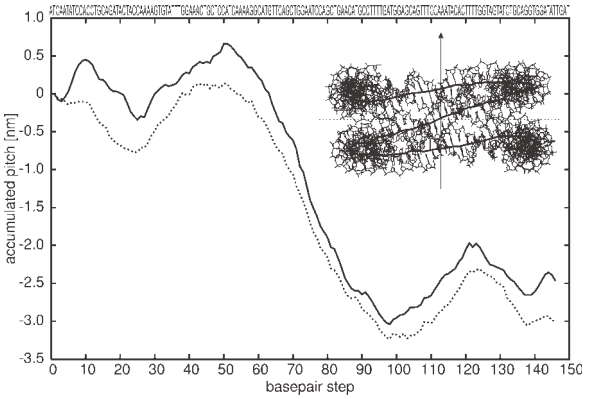

FIGURE 4 Average accumulated superhelical pitch along the nucleosomal DNA during the data gathering phase of the MD-simulation (including histone tails). For comparison, the results for the experimental X-ray start structure (pdb: 1kx5, Reference 3) is also shown (dotted line). The DNA sequence is included on top of the plot. The superhelical structure and axis system from a snapshot of nucleosomal DNA during the MD-simulations are shown in the inset of the plot. The DNA (only heavy atoms) is shown as a stick model and the DNA helical axis calculated using curves[45] is indicated as bold line. The superhelical axis (central arrow) and the mean superhelical plan (dashed line) were calculated from a principal component analysis of the deoxyribose C_1' atoms (see Materials and Methods).

simulations. This motif shows up in Figure 3 as positive peaks of the helical parameter slide coupled to negative peaks of the parameter roll. However, the average peak magnitudes in roll and slide that cause kinks are smaller during the simulation compared to the X-ray structure (Figure 3). This reduction is compensated by increased fluctuations in helical parameters around the kink sites.

Analysis of Superhelical Dynamics

In addition to the analysis of helical parameter fluctuations along the DNA, the superhelical geometry and its dynamics has been investigated. This analysis allowed us to characterize the relative motion of DNA segments (e.g. minor and major groove motion) separated by one superhelical turn of the DNA along and perpendicular to the superhelical axis. Since again the analysis of the tail-less nucleosome gave similar results on the present 20 ns time scale, only the analysis of the simulation of the complete nucleosome core particle will be presented. For each simulation frame of the data gathering phase (5–20 ns), a PCA of the deoxyribose C_1'-atoms was performed (see Materials and Methods). The eigenvector with smallest eigenvalue corresponds to a superhelical axis, whereas the other two eigenvectors define a mean plane perpendicular to the superhelical axis (Figure 4). The projection of the position of each base-pair onto the superhelical axis allows the calculation of a superhelical rise (pitch). The accumulated pitch along the superhelical axis (Figure 4) is negative (according to our definition of the direction of the superhelical axis, see Materials and Methods) and results in a total average pitch (for the complete nucleosomal DNA) of 2.52 nm in very close agreement with experiment (2.6 nm)[3] and slightly smaller than for the X-ray structure (3.0 nm). However, the contribution of each base-pair to the superhelical pitch is nonuniform (Figures 4 and 5). With respect to the current superhelical axis definition, the nucleosomal DNA may be divided into three segments to describe their superhelical structure. In this manner, it consists of two approximately coplanar superhelical half turns, bp 1–50 and 99–147, which are joined by a noncoplanar superhelical half turn from bp 51–98 contributing to the superhelical pitch predominantly (Figures 5 and 6). Minor contributions to the superhelical pitch arise from the base-pairs 10–27 and 120–137. Because of the latter, the mean planes of the coplanar half turns are not parallel to the DNA mean plane, which is based on the atomic coordinates of all C_1' atoms, but inclined with respect to the superhelical axis as illustrated in the inset of Figure 4. For that reason, the DNA segments bp 25–50 as well as bp 100–120 appear to decrease the superhelical pitch, i.e. positive values. The comparison of the pitch of one base-pair with respect to a base-pair one superhelical turn ahead versus DNA position gives an impression on the average distance of DNA segments separated by a superhelical turn and its fluctuation (Figure 5). The average pitch per turn is significantly smaller if it involves the terminal base-

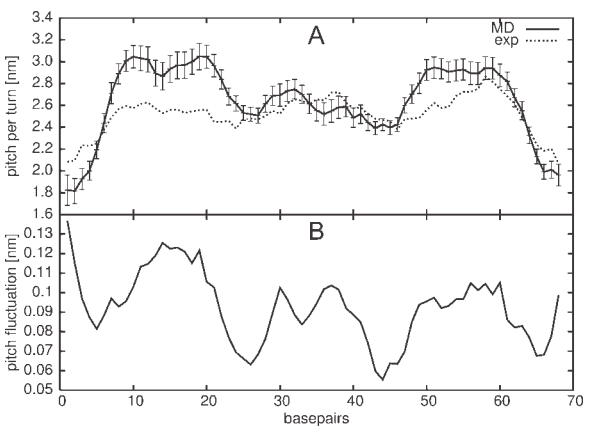

FIGURE 5 (A) Superhelical pitch of base-pairs separated by one superhelical turn along the nucleosomal DNA. The fluctuations observed during the data gathering phase of the MD-simulation (with tails) are indicated as error bars. Results for the experimental X-ray start structure (pdb: 1kx5, Ref. 3) are also indicated (dotted line). Part (B) indicates the magnitude of the fluctuations (standard deviations) of the superhelical pitch (distance along the direction of the superhelical axis) between base-pairs separated by one superhelical turn versus base-pair position.

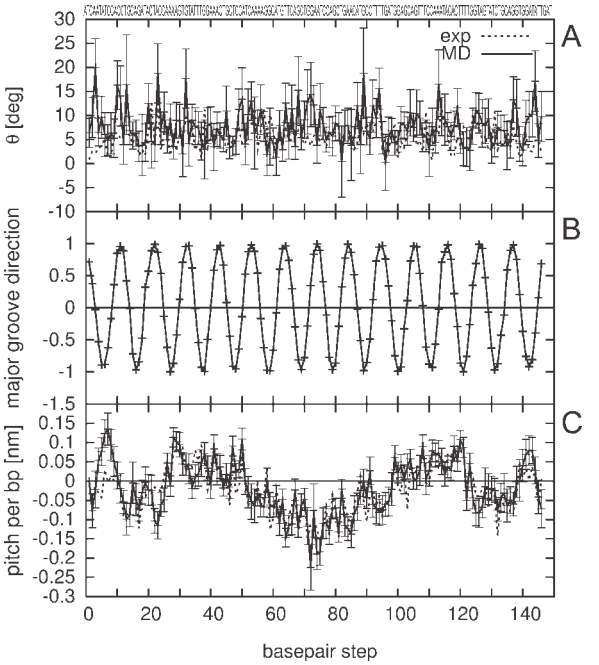

FIGURE 6 (A) Local DNA-bending θ based on normal base-pair vectors (dotted line represents X-ray start structure, 3). (B) Direction of the major groove [a negative value indicates that the major groove points outward away from the helical axis, a positive value indicates an orientation pointing toward the super helical axis (or the center of the nucleosome)]. (C) Average contribution of each base pair to the superhelical pitch of the nuclesomal DNA during the data gathering phase of the simulation (with histone tails).

pairs (also observed for the X-ray structure but not as pronounced as for the average MD result, Figure 5A). For the rest of the nucleosomal DNA, it can vary between 2.5 and 3.0 nm. The fluctuations of the mobility of DNA segments separated by one superhelical turn (in the direction of the superhelical axis, arrow in the inset of Figure 4) was between $\pm$0.06 and 0.15 nm. It is also possible to calculate the mobility of DNA segments separated by one turn with respect to the direction of the DNA helical axis (along the direction of the bold line in the inset of Figure 4). The MD simulations indicated an average fluctuation of $\pm$0.15 nm along the DNA. Dervan and coworkers have solved the structure of a nucleosome in complex with minor groove binding ligands[50] that span two spatially close minor grooves of the two turns of DNA in the nucleosome separated in sequence by $\sim$80 bp forming a "super groove." Since such super groove is well accessible, it is possible that some DNA-binding proteins explore a similar super groove binding mechanism.[50] The relative mobility of the two minor grooves with respect to each other that can form a super groove is a critical parameter that determines binding affinity of any ligand to the super groove. It also indicates that a tightly bound ligand may in turn significantly affect the DNA mobility and stabilizes and rigidifies the nucleosome structure. The current simulations indicate that at least on the nanosecond time scale rather limited motions of one groove with respect to another groove separated by one superhelical turn are possible ($\pm$0.06–0.15 nm along the superhelical axis and $\pm$0.15 nm along the direction of the helical axis). The magnitude of these motions is comparable to the free space in a DNA minor groove but considerably smaller than the size of the DNA major groove itself ($\sim$0.8 nm).

Along the nucleosomal DNA, segments with the major groove pointing away from the superhelical axis periodically interchange with major groove segments pointing toward the superhelical axis (illustrated as major groove direction in Figure 6B). Since the smooth major groove bending by roll and tilt spans several base-pair steps, the DNA helical axis does not bend planar exclusively, but also pitches with respect to the superhelical axis. To avoid DNA miswrapping around the histone core upon major groove bending and to maintain the approximate coplanarity of the two half turns bp 1–50 and 99–147, the track of DNA needs to be corrected. This is achieved in part by minor groove kinks, which are caused by positive translational slide and negative rotational roll, when the minor groove points toward the superhelical axis (Figure 3). This mechanism has been described by Tolstorukov et al.[51] in an analysis of nucleosome crystal structures. However, as indicated in Figure 6, major groove bending also contributes to the superhelical pitch at several base-pair steps. This is possible at DNA regions that show significant local bending when the major groove vector is parallel or antiparallel with the superhelical axis vector (e.g. at position where *P* in Figure 6B goes from negative to positive values or vice versa).

Figure 6A presents the local DNA-bending based on the normal base-pair vectors. In conjunction with the major groove direction along the DNA (Figure 6B), it exhibits significantly bent regions, where the major groove points toward the superhelical axis and less bend (stiff) regions, where the minor groove is directed toward the superhelical axis. The favored major groove bending is due to less introduction of mechanical stress to DNA compared to the minor groove bending that result in minor groove compression, and thus backbone repulsion. The periodicity of the groove direction correlates very well with the rotational base-pair step parameters, in particular with the roll angle (Figure 3). The DNA is mainly bent by positive roll angles, when the major groove points toward the superhelical axis. Negative roll angles, occurring when the minor groove points toward the superhelical axis, in combination with positive slide contribute to the pitch but contribute less significant to the DNA-bending around the superhelical axis.

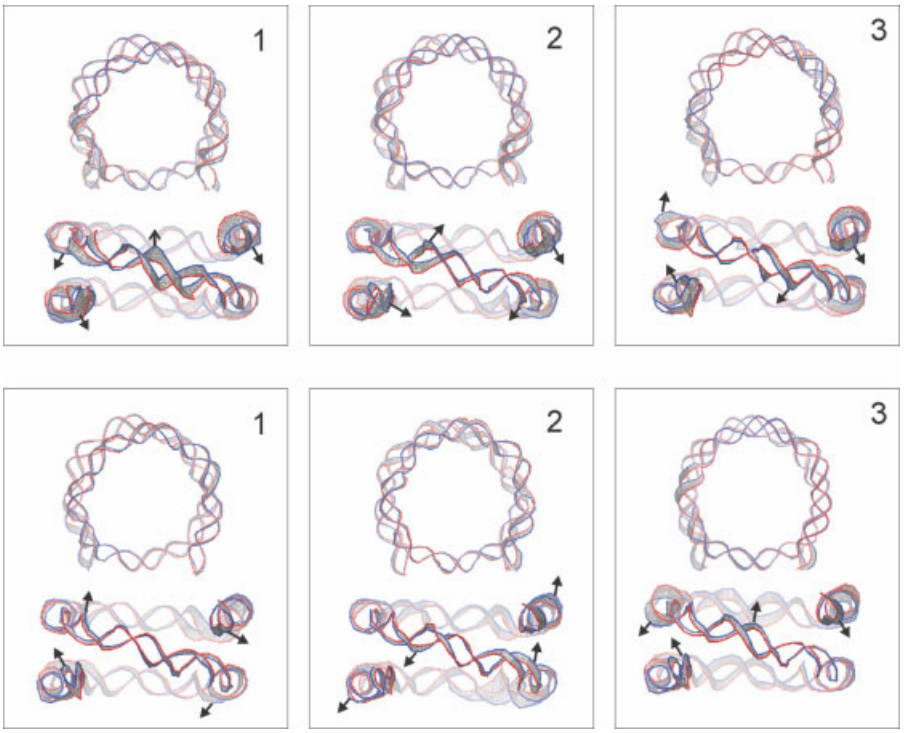

FIGURE 7 Global motion of the nucleosomal DNA. Superposition of nucleosomal DNA structures (backbone tube representation) deformed in the three softest principal components (1–3) obtained from the data gathering phase of the full nucleosome (upper three panels) and the tail-less nucleosome simulation at low salt (lower three panels). The deformation is illustrated by a superposition of several structures deformed in the respective mode. To better illustrate the collective motion of DNA segments, the maximum deformations are expanded up to three times with respect to the average deviation obtained for each mode during the simulation. The extremes of the deformations are indicated as blue and red tubes. Approximate directions of coupled motions are indicated by arrows.

Global Motions and Motions of the Ends of Nucleosomal DNA

The motion of the nucleosomal DNA during the 15 ns data gathering phases was analyzed using PCA of the covariance of sugar C_1' atom fluctuations. Except for the histone tails (see below), the histone core protein parts were less mobile than the DNA. The analysis was therefore focused on characterizing the global motion of the DNA. Control calculations indicated that the characteristic global motions described by the first ~20 softest modes did not change significantly upon inclusion of more sugar and nucleic acid backbone atoms. Presumably, this is due to the fact that deformations in the softest global modes cause only minimal relative positional changes (distances) of atoms within one nucleotide. The largest amplitude motions observed for the DNA corresponded to out-of-plane motions with respect to the plane perpendicular to the superhelical axis of the nucleosomal DNA (illustrated in Figure 7). The analysis of eigenvalues indicates that indeed a significant part of the DNA fluctuations are included in a few softest modes (~50% in 10 softest modes, Figure 2 in the Supplementary Material). The out-of-plane motions involve significant rotation (rolling) of DNA segments and coupled shifts of the location of DNA segments with respect to the second DNA turn. The motions are mostly in phase (distance between DNA of the two turns is approximately constant) or to a lesser degree out of phase (modulates the distance between DNAs of two turns). This agrees with the analysis of superhelical fluctuations (previous paragraph) that indicate a rather restricted mobility of base-pairs separated by one superhelical turn along the superhelical axis. In the softest modes, the two ends of DNA undergo the largest amplitude breathing motion of the DNA. Qualitatively, similar motions were present in the softest modes obtained during simulations of the tail-less nucleosome (Figure 7, lower panels). Recently, nucleosome dynamics has been studied using approximate normal mode analysis based on a Gaussian network model (GNM).[52] Interestingly, the softest mode obtained in this approximate normal mode

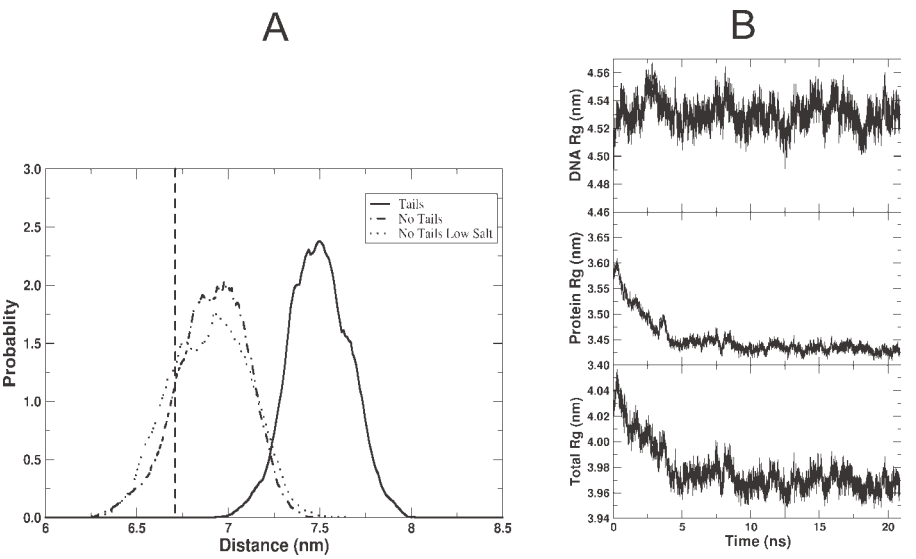

FIGURE 8 (A) Distance probability distribution of DNA ends observed during the data gathering phase of the MD simulations. (B) Radius of gyration (R_g) of DNA, histones, and complete nucleosome versus simulation time.

analysis also corresponded to an out of plane nucleosome bending motion similar to the softest modes in the present analysis. However, the GNM analysis predicted an expansion/contraction mode as second most mobile collective degree of freedom corresponding to an overall nucleosome expansion/contraction along directions perpendicular to the superhelical axis. Such globally soft mode was not observed among the softest modes in the present study most likely due to the fact that it involves either significant expansion/contraction of the histone octamer (coupled to the DNA motion) or transient disruption of DNA–histone contacts (not observed in the MD simulation). Correspondingly, also no soft flexible modes that dramatically changed the superhelical diameter or pitch could be identified.

The distance of the ends of the nucleosomal DNA fluctuated during simulations by up to $\pm$0.5 nm (Figure 8). This is larger than observed distance fluctuations between two DNA segments separated by one superhelical turn (on the same side of the nucleosome, $\pm$0.15 nm, see previous paragraph). Also, only small distance fluctuations between two DNA segments separated by one-half of a superhelical turn of $\sim\pm$0.1 nm were observed that are in line with the absence of soft degrees of freedom that expand the nucleosome in the plane perpendicular to the superhelical axis. A number of transcription factors (e.g. LexA, Amt1) are known to associate preferentially to the ends of the DNA in nucleosomes requiring partial DNA–histone dissociation at the DNA ends. The significant distance fluctuations of the DNA ends correspond to a breathing motion and increased accessibility of the DNA ends in accordance with a "site exposure model," which postulates that the ends of nucleosomes are in equilibrium between open and bound DNA conformation.[15] It is also likely that such mobile direction of motion coincide with the direction of DNA unwrapping during nucleosome dissociation.

Conformational Fluctuation and Rearrangement of Histone Tails

The overall radius of gyration (R_g) of the nucleosome (DNA and protein) decreased during the first 5 ns of the simulation (Figure 10B). However, this is mainly due to changes in the proteins, whereas the radius of gyration of the DNA alone did not show any appreciable changes (Figure 8B). The calculated $R_g = 4.53$ nm is in good agreement with experimental data ($R_g = 4.4$–4.5 nm, 42). In contrast to the histone core parts, the N-terminal tails do not stay close to the crystallographic starting placement where the tails in part contact neighboring nucleosomes in the crystal.[3,4] Instead, large conformational readjustments of the histone tail segments were observed to states with part of the tails associated with the minor and major grooves on the exposed side of the DNA (Figures 9 and 10). This was accompanied by a significant reduction of the solvent accessible surface during the simulation from $\sim$900 nm^2 to $\sim$885 nm^2 at the end of the simulation. The reduction by 15 nm^2 is similar to the average reduction seen during protein–protein or protein–DNA complex formation. The contribution of the surface area reduction of the histone proteins (mainly the histone tails) amounted to $\sim$6 nm^2 ($\sim$9 nm^2 for the DNA). It indicates the

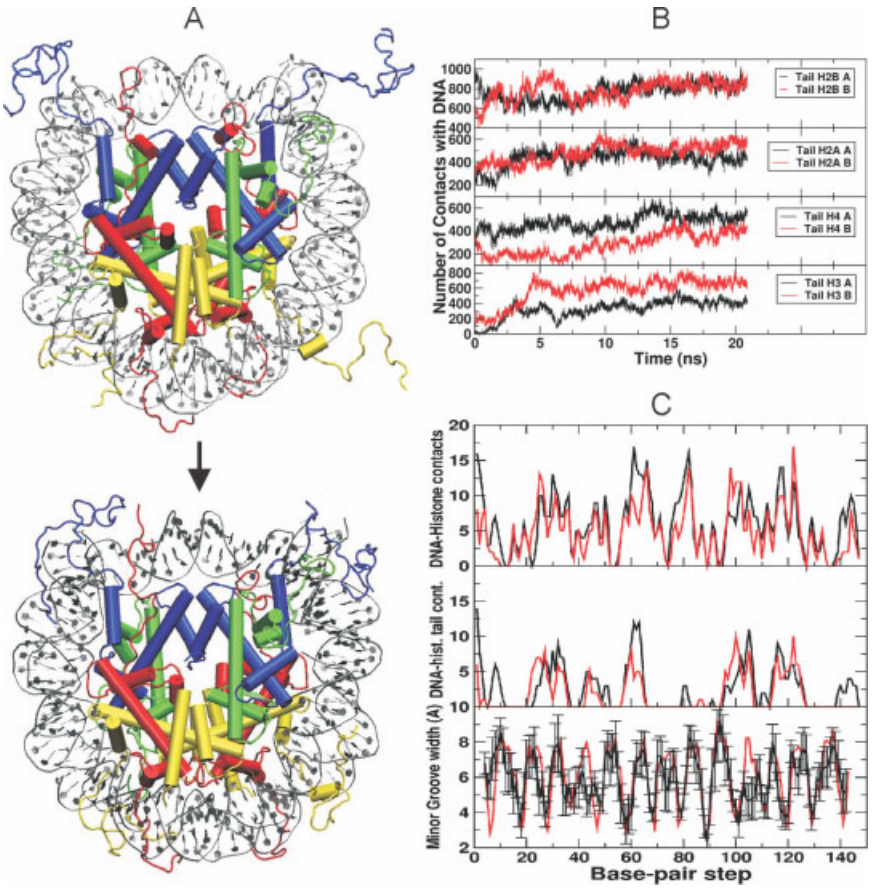

FIGURE 9 Histone tail motion and accessibility of nucleosomal DNA during MD simulation. (A) Comparison of histone tail conformations (snapshot) after ~1 ns simulation time (upper panel) and after ~21 ns (final snapshot). The histone proteins are represented as colored tube models (red: histone H2A; yellow: H2B; blue: H3; green: H4) and the DNA as a cartoon model (grey). (B) Time course of the number of DNA–histone tail contacts during MD simulation of the full nucleosome structure. (C) The upper two panels indicate the number of DNA–histone and DNA–histone tail contacts, respectively, in the X-ray structure (red) and at the final stage of the simulation (black curve). Two (heavy) atoms are considered in contact if the atom–atom distance is <0.4 nm. Panel 3 compares the minor groove width of the start (red) and final structures (black) of the simulation, respectively.

tendency of the nucleosome to adopt a more compact and solvent-protected structure during the simulation. The structural change is mainly promoted by the diffusive motion of the histone tails from a solvent-exposed conformation to conformations in partial contact to DNA (DNA-wrapped conformations). The partial wrapping of histone tails during the simulation at physiological salt concentration contradicts experimental findings that indicate that the histone tails adopt a largely solvent-exposed structure at salt concentrations above ~100 m*M*.[28] Only at salt concentrations below 50 m*M* the nucleosome forms a compact structure with the tails presumably wrapped around DNA.[28] It is well known that periodic boundary conditions and lattice sum techniques to treat long range electrostatic interactions in charged biomolecular systems artificially "overstabilize" compact states of biomolecules during MD simulations.[53,54] The compact nucleosome solution conformations observed in the present simulation study may therefore be more representative of the nucleosome structure observed experimentally under low salt conditions (<50 m*M*[28]). One should, however, keep in mind that wrapped DNA-bound histone tail conformations may correspond only to intermediate wrapped states that on much longer time scales than the present 20 ns dissociate from DNA and fluctuate between exposed and bound states. The most significant conformational change was observed for the histone H3 tails with respect to the initial structure. In the initial structure, the H3 tails are solvent-exposed and partially contact neighboring

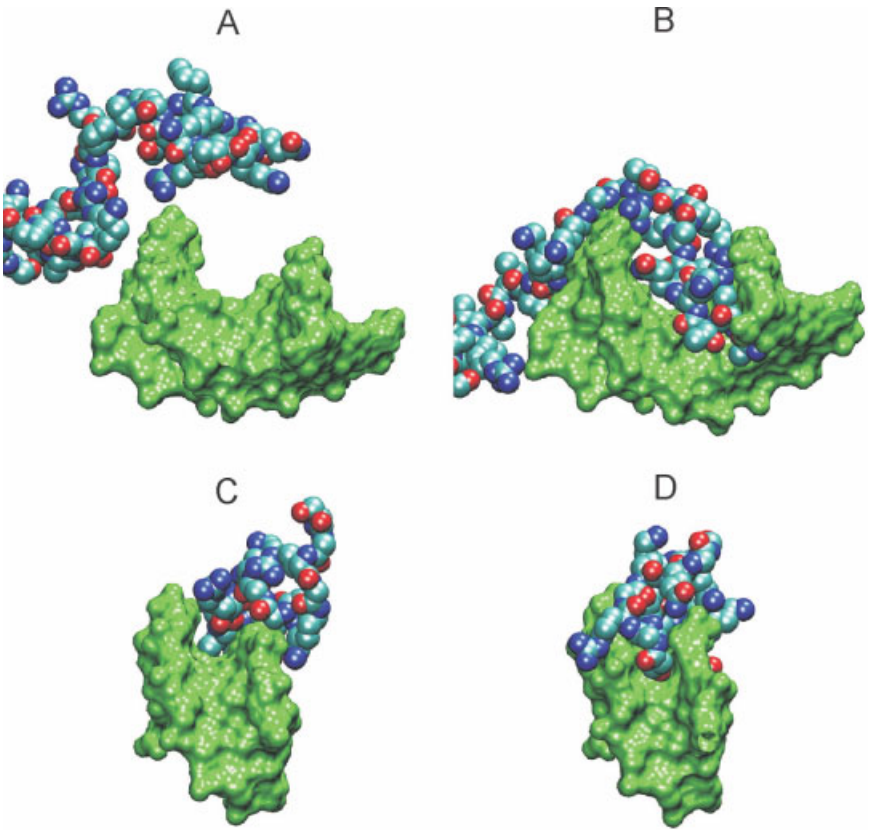

FIGURE 10 Histone tail–DNA contact formation during MD simulation. (A) Snapshot of N-terminal histone H3 tail (residues 1–26, van der Waals representation in atom color code) and nucleosomal DNA major groove (first 10 bp, green molecular surface) at ~2 ns simulation time. (B) Same as (A) but at 21 ns simulation time. (C) Snapshot of the N-terminal histone H2A tail (residues 1–12, van der Waals representation) and DNA minor groove (base-pairs 112–118, green surface) at ~2 ns simulation time and at 21 ns (D).

nucleosome particles in the crystal.[3] During the simulation, the tails started to wrap around the respective ends of the DNA chain and intercalated into the DNA major grooves near both ends of the nucleosomal DNA. In this case also a significant increase in the number of close DNA–tail contacts was observed (Figure 9B). Here, two heavy atoms are defined to be in contact if the atom–atom distance is less than 0.4 nm. The tail conformation of one H3 protein and its contacts to DNA at an initial phase of the simulation (~2 ns) and during the final stage (~20 ns) are illustrated in Figure 10. A transition from a stage with no contacts between tails and DNA to a conformation where the tail largely fills out the major groove was observed. This structural transition corresponds to coupled association and folding event of a histone tail starting from a solvent-exposed structure to a DNA-bound structure with multiple protein–DNA interactions. Some of the new interactions are also water-mediated. Similar to the major groove, increased H2A tail-association with the DNA minor groove was also observed (Figures 10C and 10D). In both cases, a reduction in the groove width accompanied the conformational transition of the histone tails and DNA association. These examples illustrate that transient association of the tail region with DNA can protect the DNA grooves (and also tails) from access to other proteins. Typical contacts formed during the simulation are polar interactions between positively charged side chains and polar and charge groups of the DNA. The type of contacts are similar to the type of polar interactions between tails and DNA of neighboring nucleosomes in the nucleosome crystal structure, which also include tail phosphate and tail groove interactions.[4] Presumably, the transient nature of the contacts indicates that the histone tail–DNA interactions are typical for nonspecific protein–DNA interactions. A detailed analysis of the various types and lifetimes of interactions will be subject of a future study. The C-terminal tails of the two copies of histone protein H2A adopt a different conformation in the X-ray start structure (only one contacts DNA: chain A). During the MD simulation, the C-terminal tail that already con-

tacted DNA in the start structure increased the number of contacts (similar to the N-terminal tails), whereas the other C-terminal tail stayed in a solvent-exposed conformation. A significant increase of contacts between DNA and H4 tails was observed during the simulation although not accompanied by a large rearrangement of the tail conformation. A large diffuse motion was observed for the tail of the second H2B histone toward the space in between two superhelical DNA turns. The transient association of histone tails with the DNA affected in many cases the local DNA structure resulting, for example, in a shrinking of the DNA minor groove at several regions along the DNA (Figure 9C). As expected, the minor and major grooves on the inner side of the DNA side (in contact with the histone octamer) are generally smaller than that on the solvent-exposed side. A similar trend was observed for the fluctuations of the minor (and major groove) widths. On the exposed side, the width of the minor groove fluctuated by up to 0.3–0.4 nm compared to ~0.2 nm on the histone-facing side (Figure 9C). The large observed conformational fluctuations and fluctuations of DNA–tail contacts indicate that the transient nature may be of functional importance to create a balance between protection and accessibility for DNA-binding proteins. However, the simulation times are too short to derive statistically meaningful data on the average degree of DNA protection by the histone tails. Interestingly, the average DNA end-to-end distance is smaller in case of the tail-less nucleosome simulations (Figure 8A). Presumably, the presence of the positively charged histone tail regions at the solvent-exposed side of the DNA causes an overall attraction of the DNA to increase the average distance between the DNA ends. During both simulations without tails a slight (~5%) increase of R_g (DNA) along the superhelical axis was observed corresponding to a slight increase of the superhelical pitch. It is likely that the absence of the positively charged histone tails causes an increase of the electrostatic repulsion between the two superhelical turns of the DNA that lead to an on average slightly larger distance between the two DNA turns (Figure 8A). It is known that removal of histone tails interferes with the association and packing of nucleosomes to form chromatin-like higher order structures.[5–7,17,55] It is assumed that histone tails could mediate and stabilize association of nucleosomes by forming contacts between histone tails and DNA of neighboring nucleosomes. However, it is also possible that the loss of histone tails (or its chemical modification) leads to small global structural changes as seen in the present simulations that modulate the association tendency of nucleosomes. Such structural changes of tail-less nucleosome core particles are supported by hydrodynamic and X-ray scattering experiments.[55]

CONCLUSIONS

The goal of the present study was to analyze the nucleosomal DNA and histone dynamics on the nanosecond scale in a state characteristic for eukaryotic chromosomal DNA using MD simulations. Most previous MD studies focused on studying the dynamics of isolated DNA oligonucleotides and gave valuable insights into the fine structure of DNA, transitions toward noncanonical backbone conformations, and the helical mobility that can be observed on the nanosecond time scale.[48,49] But the dynamic behavior of DNA may change in its more "natural" environment where the DNA is packed in nucleosomes in a bend conformation and possessing a highly asymmetric groove structure. However, in the present simulation study, no increase in transition frequencies of the nucleic backbone toward noncanonical states has been observed due to the packing strain in the nucleosome. Recent experimental and computational studies indicate the possibility of spontaneous sharp bending and kinking of DNA in minicircles.[24,45] During the present simulations, the pattern of local helical parameters stayed overall close to the experimental nucleosome structure[3] indicating no rapid exchange with alternative bending or kinking patterns along the DNA. Electrostatic interactions and water molecules mediate many of the histone–DNA interactions. Nucleosome remodeling requires the transient dissociation of the histone–DNA complex, which corresponds to the simultaneous disruption of many contacts. A rapid transient local dissociation of histone–DNA contacts might be compatible with the long-range nature of the electrostatic interactions and the solvent-accessibility of histone–DNA interface.

However, on the time scale of the current MD simulations neither in case of the tail-less nor for the full nucleosome, a disruption of histone–DNA contacts has been observed. Increased mobility of the DNA termini and significant distance fluctuations of the DNA ends observed during the simulation are compatible with the hypothesis that DNA unwrapping starts from the DNA ends and not spontaneously at more central regions of nucleosomal DNA. A slight (5%) expansion of the DNA in case of the tail-less nucleosome simulations was observed presumably because the positively charged histone tails neutralizes the negatively charged DNA allowing a larger compactness of the nucleosome.

The crystal structure of the nucleosome allowed us to determine the exact superhelical geometry of the nucleosome, however, from the crystal structure alone it is also not possible to extract information on the superhelical DNA mobility in the nucleosome. This information is of importance for understanding the larger scale packing of nucleosomes and for the development of simplified dynamical models of

nucleosomes and chromatin structures (coarse grained models). On the present MD timescale, the superhelical geometry of the nucleosome was surprisingly rigid. Only very limited variation in the relative position of DNA segments separated by one half of a superhelical turn were observed ($\sim\pm0.1$ nm). Also, the overall superhelical pitch (motions along the superhelical axis) fluctuated by only $\sim\pm0.2$ nm. This result is of importance for understanding and design of protein- or ligand-binding that involves more than one superhelical turn in nucleosomal DNA.[50]

In contrast to the close agreement of the nucleosome core structure with the X-ray start structure, the histone tails underwent significant conformational changes from extended structures to states partially wrapped around the DNA. Significant mobility of these segments was expected but the degree of rearrangement on the current simulation time scale was unexpected. Multiple coupled association and folding transitions of the histone tails to complexes that filled major and minor grooves of DNA were observed. However, the predicted more compact nucleosome structure at physiological salt concentration observed during the simulation contradicts small angle X-ray studies that indicated solvent exposed histone tails at approximately the same salt concentration.[28] A possible reason for this discrepancy might be an artificial "overstabilization" of compact biomolecular structures due to the present simulation conditions employing periodic boundary conditions and a lattice sum method (PME) to account for long range electrostatics.[53,54] Alternatively, the tail conformations seen on the present time scale may represent only a small fraction of possible structures that include also many solvent-exposed states on longer time scales. The transient nature of the observed DNA–tail contacts is supported by the observation that no single or symmetric DNA protection pattern with respect to the two histone copies was found. The observed large scale rearrangement of histone tails during the simulations indicates that the transient changes in the accessibility of the histone tails may also influence the recruitment and binding of regulatory proteins. The current simulation studies may form a basis for future studies on larger structural changes such as DNA unwrapping from the histone octamer by enforcing such changes during MD simulations that could be of great importance to understand nucleosome mobility and remodeling at atomic detail.

This study was performed using the computational resources of the CLAMV (Computational Laboratories for Animation, Modeling and Visualization) at International University Bremen and supercomputer resources of the EMSL (Environmental Molecular Science Laboratories) at the PNNL (Pacific Northwest National Laboratories).

REFERENCES

1. Luger, K.; Maeder, A. W.; Richmond, R. K.; Sargent, D. F.; Richmond, T. J. Nature 1997, 389, 251–259.
2. White, C. L.; Suto, R. K.; Luger, K. EMBO J 2001, 20, 5207–5218.
3. Richmond, T. J.; Davey, C. A. Nature 2003, 423, 145–150.
4. Davey, C. A.; Sargent, D. F.; Luger, K.; Maeder, A. W.; Richard, T. J. J Mol Biol 2003, 319, 1097–1106.
5. Van Holde, K. E. In Chromatin; Springer: New York; 1988; p 288.
6. Fletcher, T. M.; Hansen, J. C. Crit Rev Eukaryot Gene Expr 1996, 6, 149–188.
7. Kornberg, R. D.; Lorch, Y. Cell 1999, 98, 285–294.
8. Richmond, T. J.; Widom, J. Nucleosome and Chromatin Structure; Oxford University Press: Oxford, 2000.
9. Felsenfeld, G.; Groudine, M. Nature 2003, 421, 448–453.
10. Kornberg, R. D.; Lorch, Y. Annu Rev Cell Biol 1992, 8, 563–587.
11. Anderson, J. D.; Thastrom, A.; Widom, J. Mol Cell Biol 2002, 20, 7147–7157.
12. Fazzio, T. G.; Tsukiyama, T. Mol Cell 2003, 12, 1333–1340.
13. Sivolob, A.; Prunell, A. Philos Transact A Math Phys Eng Sci 2004, 362, 1519–1547.
14. Li, G.; Widom, J. Nat Struct Mol Biol 2004, 11, 763–769.
15. Li, G.; Levitus, M.; Bustamante, C.; Widom J. Nat Struct Mol Biol 2005, 12, 46–53.
16. Lachner, M.; O'Sullivan, R. J.; Jenuwein, T. J Cell Sci 2003, 116, 2117–2124.
17. Cosgrove, M. S.; Boeke, J. D.; Wolberger C. Nat Struct Mol Biol 2004, 11, 1037–1043.
18. Khorasanizadeh, S. Cell 2004, 116, 259–272.
19. Turner, B. M. Nat Struct Mol Biol 2005, 12, 110–112.
20. Brower-Toland, B.; Wacker, D. A.; Fulbright, R. M.; Lis, J. T.; Kraus, W. L.; Wang, M. D. J Mol Biol 2005, 346, 135–146.
21. Fan, H. Y.; He, X.; Kingston, R. E.; Narlikar, G. J Mol Cell 2003, 11, 391–403.
22. Widom, J. Q. Rev Biophys 2001, 34, 269–324.
23. Segal, E.; Fondufe-Mittendorf, Y.; Chen, L.; Thaström, A.; Field, Y.; Moore, I. K.; Wang, J. Z.; Widom, J. Nature 2006, 442, 772–778.
24. Cloutier, T. E.; Widom, J. Proc Natl Acad Sci USA 2005, 102, 3645–3650.
25. Lankas, F.; Lavery, R.; Maddocks, J. H. Structure 2006, 10, 1527–1534.
26. Bishop, T. C. J. J Biomol Struct Dyn 2005, 22, 673–685.
27. Ruscio, J. Z.; Onufriev, A. Biophys J 2006, 91, 4121–4132.
28. Mangenot, S.; Leforestier, A.; Vachette, P.; Durand, D.; Livolant, F. Biophys J 2002, 82, 345–356.
29. Beard, D. A.; Schlick, T. Biophys J 2001, 9, 105–114.
30. Wedemann, G.; Langowski, J. Biophys J 2002, 2, 2847–2859.
31. Bharath, M. M. S.; Chandra, N. R.; Rao, M. R. S. Nucleic Acids Res 2003, 31, 4264–4274.
32. Mergell, B.; Everaes, R.; Schiessel H. Phys Rev E Stat Nonlin Soft Matter Phys 2004, 70, 011915.
33. Sun, J.; Zhang, Q.; Schlick, T. Proc Natl Acad Sci USA 2005, 102, 8180–8185.
34. Arya, G.; Zhang, Q.; Schlick, T. Biophys J 2006, 91, 133–150.
35. Sharma, S.; Ding, F.; Dokhalyan, N. V. Biophys J 2007, 92, 1457–1470.

36. Doublie, S.; Tabor, S.; Long, A. M.; Richardson, C. C.; Ellenberger, T. Nature 1998, 391, 251–258.
37. Cramer, P.; Bushnell, D. A.; Fu, J.; Gnatt, A. L.; Maier-Davis, B.; Thompson, N. E.; Burgess, R. R.; Edwards, A. M.; David, P. R.; Kornberg, R. D. Science 2000, 288, 640–649.
38. Case, D.; Pearlman, D. A.; Caldwell, J. W.; Cheatham, T. E., III; Ross, W. S.; Simmerling, C. L.; Darden, T. A.; Merz, K. M.; Stanton, R. V.; Cheng, A. L.; Vincent, J. J.; Crowley, M.; Tsui, V.; Radmer, R. J.; Duan, Y.; Pitera, J.; Massova, I.; Seibel, G. L.; Singh, U. C.; Weiner, P. K.; Kollman, P. A. Amber 8, University of California, San Francisco, 2003.
39. Jorgensen, W.; Chandrasekhar J.; Madura J.; Impey R.; Klein M. J Chem Phys 1983, 79, 926–935.
40. Duan, Y.; Wu A.; Chowdhury, C. S.; Lee, M. C.; Xiong, G.; Zhang, W.; Yang, R.; Cieplak, P.; Luo, R.; Lee, T.; Caldwell, J.; Wang, J.; Kollman P. J Comput Chem 2003, 24, 1999–2012.
41. Miyamoto, S.; Kollman, P. A. J Comput Chem 1992, 13, 952–962.
42. Darden, T. A.; York, D. M.; Pedersen L. J Chem Phys 1993, 98, 10089–10092.
43. Van der Spoel, D.; Lindahl, E.; Hess, B.; Groenhof, G.; Mark, A. E.; Berendsen H. J. E. J Comput Chem 2005, 26, 1701–1718.
44. Humphrey, W.; Dalke, A.; Schulten, K. J Mol Graph 1996, 14, 33–38.
45. Lavery, R.; Sklenar, H. J Biomol Struct Dyn 1988, 6, 63–91.
46. Rosenberg, J. M.; Seeman, N. C.; Day, R. O.; Rich A. Biochem Biophys Res Commun 1976, 69, 979–987.
47. Packer, M. J.; Hunter C. A. J Mol Biol 1998, 280, 407–420.
48. Dixit S. B.; Beveridge, D. L.; Case, D. A.; Cheatham, T. E., III; Giudice, E.; Lankas, F.; Lavery, R.; Maddocks, J. H.; Osman, R.; Sklenar, H.; Thayer, K. M.; Varnai, P. Biophys J 2005, 89, 3721–3740.
49. Barone, F.; Lankas, F.; Spackova, N.; Sponer, J.; Karran, P.; Bignami, M.; Mazzei, F. Biophys Chem 2005, 118, 31–41.
50. Suto, R. K.; Edayathumangalam, R. S.; White, C. L.; Melander, C.; Gottesfeld, J. M.; Dervan, P. B.; Luger, K. J Mol Biol 2003, 326, 371–380.
51. Tolstorukov, M. Y.; Colasanti, A. V.; McCandlish, D.; Olson, W. K.; Zhurkin, V. B. J Biomol Struct Dyn 2005, 22, 854–855.
52. Ramaswamy, A.; Bahar, I.; Ioshikhes, I. Proteins 2005, 58, 683–696.
53. Hünenberger, P. H.; McCammon, J. A. Biophys Chem 1999, 78, 69–80.
54. Kastenholz, M. A.; Hünenberger, P. H. J Chem Phys 2006, 124, 124108.
55. Bertin, A.; Leforestier, A.; Durand, D.; Livolant, F. Biochem 2004, 43, 4773–4780.

Reviewing Editor: David Case